

How a Nonequilibrium Bath and a Potential Well Lead to Broken Time-Reversal Symmetry - First Order Corrections on Fluctuation-Dissipation Relations

Steven Yuwan ^{1,†}, Nick Bellardini ^{2,†} and Martin Bier ^{1,3,†,*} 

¹ Dept. of Physics, East Carolina University, Greenville, NC 27858

² Dept. of Mathematics, East Carolina University, Greenville, NC 27858

³ Faculty of Mechanical Engineering and Institute of Mathematics and Physics, University of Technology and Life Sciences, 85-796 Bydgoszcz, Poland

* Correspondence: bierm@ecu.edu

† These authors contributed equally to this work.

Abstract: The noise that is associated with nonequilibrium processes commonly features more outliers and is therefore often taken to be Lévy noise. For a Langevin particle that is subjected to Lévy noise, the kicksizes are drawn not from a Gaussian distribution, but from an α -stable distribution. For a Gaussian-noise-subjected particle in a potential well, microscopic reversibility applies. But it appears that the time-reversal-symmetry is broken for a Lévy-noise-subjected particle in a potential well. Major obstacles in the analysis of Langevin equations with Lévy noise are the lack of simple analytic formulae and the infinite variance of the α -stable distribution. We propose a measure for the violation of time-reversal-symmetry and we present a procedure in which this measure is central to a controlled imposing of time-reversal-asymmetry. The procedure leads to behavior that mimics much of the effects of Lévy noise. Our imposing of such nonequilibrium leads to concise analytic formulae and does not yield any divergent variances. Most importantly, the theory leads to simple corrections on the Fluctuation-Dissipation Relation.

Keywords: Fluctuation-Dissipation Relation; Lévy Noise; Nonequilibrium; Time Reversal Symmetry Breaking

Citation: Lastname, F.; Lastname, F.; Lastname, F. Title. *Symmetry* **2021**, *1*, 0. <https://doi.org/>

Received:
Accepted:
Published:

Publisher's Note: MDPI stays neutral with regard to jurisdictional claims in published maps and institutional affiliations.

Copyright: © 2022 by the authors. Submitted to *Symmetry* for possible open access publication under the terms and conditions of the Creative Commons Attribution (CC BY) license (<https://creativecommons.org/licenses/by/4.0/>).

1. Introduction

The Fluctuation-Dissipation Relation (FDR) is as simple as it is profound [1]. For a particle in a fluid we have

$$D/(k_B T) = \mu. \quad (1)$$

On the left hand side of this equation, D is the diffusion coefficient of the particle, k_B is Boltzmann's constant, and T is the absolute temperature. The product $k_B T$ has the dimension of energy and it is the characteristic "quantum" of Brownian motion. On the right hand side μ denotes the mobility, i.e., $\mu = v/F$ where v is the average speed of the particle in the fluid when it is subjected to a force F .

On the molecular level there are other manifestations of the FDR. Take a resistor with a conductance G . With no net current flowing, there is still a fluctuating voltage between the two ends of the resistor due to the Brownian motion of the charge carriers (generally electrons) inside the resistor. Conductance can be viewed as the electrical equivalent of mobility, i.e. $G = I/V$ with V being the voltage and I being the current. With this realization it is not hard to understand that the mean square of the fluctuating current, $\langle I^2 \rangle$, is related to the conductance G through $k_B T$. The relation $\langle I^2 \rangle = 4k_B T G(\Delta f)$, where Δf is the frequency window, is known as the Johnson-Nyquist relation [2].

Thinking of it more abstractly, the FDR connects characteristics of internal fluctuations on the left hand side of Eq. (1) with a first-order, linear response to external

31 prompting on the right hand side of Eq. (1). The equation relates the first moment upon
 32 application of a perturbing force to the second moment in the absence of such a force. A
 33 more all-encompassing formulation of the FDR is due to Green and Kubo [3].

34 For the FDR to apply, it is essential that the system is close to equilibrium. Equi-
 35 librium means that there is no identifiable arrow of time. A system at equilibrium
 36 displays time-reversal symmetry. About a century ago Lars Onsager formulated the
 37 notion of microscopic reversibility, which is short for “time reversibility of microscopic
 38 dynamics” [4,5]. It means that any trajectory in a configuration space from an initial
 39 point (t_{ini}, x_{ini}) to a final point (t_{fin}, x_{fin}) is traversed in one direction as often as it is
 40 in the opposite direction. Much of the first order theory that describes systems that
 41 are close-to-equilibrium, like Onsager’s reciprocal relation for coupled energy flows, is
 42 based on the idea that microscopic reversibility still applies in case of small deviation
 43 from equilibrium [4,5].

44 Considerable research effort has been directed towards formulating an FDR for
 45 a system that is far away from equilibrium. In the late 1990s, the Jarzynski Equation
 46 gave insight into the response of a system when nonequilibrium is imposed beyond a
 47 regime where linear perturbation theory applies [6,7]. The Jarzynski Equality has an
 48 elegant simplicity and soon after its discovery it also turned out remarkably accurate
 49 in quantitatively accounting for the results of micromanipulation experiments with
 50 biomolecules [8].

51 The work towards a nonequilibrium FDR has commonly taken an approach that
 52 is similar to the one that led to the Jarzynski Equation [9,10]. The guiding idea has
 53 been to let nonequilibrium events happen in a bath that is at equilibrium and that has a
 54 temperature. Temperature is a collective property and actually only makes sense if the
 55 collective is at equilibrium.

56 But what if the bath is the very source of nonequilibrium?

57 In liquid water at room temperature an individual water molecule collides about
 58 10^{12} times per second. For time intervals Δt that are significantly larger than a picosecond
 59 the displacement of such a water molecule is the result of many collisions. The Central
 60 Limit Theorem [1] applies in that case and the displacement in Δt follows the Gaussian
 61 distribution that is associated with equilibrium.

62 Through numerical simulation Kanazawa et al. recently showed that in active
 63 media, i.e. media with artificial self-propelled colloids or swimming microorganisms,
 64 displacements of passive tracers follow, not a Gaussian, but an α -stable distribution [11].

Where a Gaussian distribution results for a process that is the cumulative effect
 of stochastic processes with a *finite* standard deviation, an α -stable distribution results
 when *infinite* standard deviations come into play. The analytic expression for the α -stable
 distribution is huge and cumbersome, but in Fourier space a concise formula ensues.
 For a symmetric, zero-centered α -stable distribution the generating function is:

$$\tilde{p}_\alpha(k) = \exp[-c^\alpha |k|^\alpha]. \quad (2)$$

65 Here c is a scale factor and α is the so-called stability index ($0 < \alpha \leq 2$). For $\alpha = 2$ the
 66 Gaussian distribution is actually retrieved and for $\alpha = 1$ the α -stable distribution is the
 67 simple and well-known Cauchy distribution, i.e. $p(x) = (c/\pi)(c^2 + x^2)^{-1}$.

68 Nonequilibrium is commonly characterized by frequently occurring “outliers” [12–
 69 17]. If “outliers” means a Brownian trajectory with an overabundance of very large steps,
 70 then replacing the Gaussian distribution by an α -stable distribution is the next sensible
 71 move in the modeling.

72 It is in the asymptotics, i.e. the behavior at $|x| \rightarrow \infty$, that we find the most salient
 73 difference between a Gaussian and an α -stable distribution. For the Gaussian distribution
 74 the convergence follows $p(x) \sim \exp[-x^2/4c^2]$ and is rapid (Note here that for $\alpha = 2$,
 75 the scale factor c is the standard deviation divided by $\sqrt{2}$). For the α -stable distribution
 76 the tail follows a power law: $p(x) \sim |x|^{-\alpha-1}$. The slow convergence of the power law tail

77 leads to an infinite standard deviation and is also behind the more frequent occurrence
78 of outliers [18,19].

79 2. Overdamped Particle in a Potential Well Subjected to IID α -stable Noise

Consider a particle in a potential $V(x)$ that is subjected to α -stable noise. We have for the Langevin Equation for the position $x(t)$ of an overdamped particle:

$$\beta\dot{x} = -\frac{dV(x)}{dx} + \beta c\zeta_\alpha(t). \quad (3)$$

In the course of a simulation with timesteps of length Δt , a noise contribution $\zeta(t_i)$ at the i -th step is taken as $\zeta_\alpha(t_i) = \theta_{\alpha,i}\Delta t^{1/\alpha-1}$, where $\theta_{\alpha,i}$ is the i -th random number in the sequence of steps. The random numbers $\theta_{\alpha,i}$ are drawn from an α -stable distribution with a scale factor of one. They are independent and identically distributed (IID). The $1/\alpha$ in the exponent of Δt guarantees that the diffused distance scales correctly if different Δt 's are taken. Equation (3) furthermore shows how the scale factor is effectively an amplitude. For Gaussian noise, i.e. $\alpha = 2$, the scale factor c is the usual $\sqrt{2D}$, where D is the diffusion coefficient. The variable β denotes the coefficient of friction. The coefficient of friction is the inverse of the aforementioned mobility μ , i.e. $\beta = 1/\mu$. The left- and right-hand-side of Eq. (3) have the dimension of force. We consider a small segment of a trajectory going from (t_i, x_i) to $(t_i + \Delta t, x_i + \Delta x_i)$. Multiplying with Δx_i , we obtain the involved energies: $\beta\left(\frac{\Delta x_i}{\Delta t}\right)\Delta x_i = [F(x_i) + \beta c\zeta_\alpha(t_i)](\Delta x_i)$. Here the term on the left-hand-side indicates the amount of energy that is "dissipated out" in time Δt . The term in square brackets on the right-hand-side denotes the net force on the particle. The net force is made up of the force due to the potential, $F(x_i) = -dV(x_i)/dx$, and the force due to agitation by the bath. Multiplying the net force by the distance Δx_i over which the force is applied, we obtain the work done on the particle over the segment Δx_i . Writing $F(x_i)\Delta x_i = -V(x)|_{x_i}^{x_{i+1}}$, substituting $\Delta x_i = [F(x_i)/\beta + c\zeta_\alpha(t_i)]\Delta t$ on the right-hand-side, and using again $\zeta_\alpha(t_i) = \theta_{\alpha,i}\Delta t^{1/\alpha-1}$, we find:

$$\beta\frac{(\Delta x_i)^2}{\Delta t} + V(x)|_{x_i}^{x_{i+1}} = cF(x_i)\theta_{\alpha,i}\Delta t^{1/\alpha-1} + \beta c^2\theta_{\alpha,i}^2\Delta t^{2/\alpha-1}. \quad (4)$$

80 This equation again describes the energy traffic for the particle in a time interval Δt .
81 On the left-hand-side the first term is the dissipated energy and the second term is the
82 energy associated with going up or down in the potential. The twofold expression on the
83 right-hand-side describes the energy that is "fluctuated into the particle." The second
84 term would be the only contribution in case of a flat potential. The first term accounts
85 for the interplay between the random kicks, $\zeta_\alpha(t_i)$, and the deterministic $F(x_i)$. If the
86 Brownian kick and the deterministic force are in the opposite direction and such that
87 they balance each other out, then the right-hand-side terms in Eq. (4) will add up to zero
88 and the particle will not move.

For the case of $\alpha = 2$, Eq. (4) readily reduces to something more familiar. On the left-hand-side, the existence of a basin of attraction implies that the changes $V(x)|_{x_i}^{x_{i+1}}$ will ultimately average to zero. Furthermore, we have $\langle\theta_{2,i}\rangle = 0$ and $\langle F(x_i)\rangle = 0$ in this case. As the kick sizes $\theta_{2,i}$ are not correlated to $F(x_i)$, we also have $\langle F(x_i)\theta_{2,i}\rangle = 0$ on the right-hand-side. The Gaussian case, $\alpha = 2$, also leads to $\langle\theta_{2,i}^2\rangle = 1$. With $c^2 = 2D$ and invoking the FDR, $\beta D = k_B T$, we then obtain:

$$\beta\langle\dot{x}^2\rangle = \frac{2k_B T}{\Delta t}. \quad (5)$$

89 This equation tells us that the long time average of the energy that is fluctuated into
90 the particle is $2k_B T$ per timestep. Note that in the continuum limit, $\Delta t \rightarrow 0$, an infinite
91 amount of energy flows through each particle in the system in any finite amount of time.
92 The Langevin Equation, however, is an abstraction. As was mentioned before, in actual

93 reality there is about a picosecond between subsequent collisions of an individual water
 94 molecule and this puts a lower limit on the value of Δt . Equation (5) has proven fruitful
 95 in the analysis of Brownian ratchets [20,21].

96 A lot more infinities start accumulating once we make $\alpha < 2$. For $0 < \alpha < 2$, the
 97 variance $\langle \theta_{\alpha,i}^2 \rangle$ diverges. Effectively this means that the bath has no temperature. No
 98 FDR can be formulated in this case. For $0 < \alpha \leq 1$, $\langle \theta_{\alpha,i} \rangle$ is zero-centered, but does
 99 not converge. This leads to further problems in working with Eq. (4). However, most
 100 real-life instances of Lévy noise involve values of α that are between 1 and 2 [12–17].

101 Below we propose a way to “fix” the $\langle \theta_{\alpha,i}^2 \rangle$ -divergence for small deviations from
 102 equilibrium. The idea is inspired by the violation of time-reversal-symmetry that Lévy
 103 noise causes for a particle in a potential well. We will derive some simple formulae that
 104 we will check against the results of numerical simulation.

105 3. Nonequilibrium and Time-Reversal Asymmetry in a Parabolic Well

106 If $V(x)$ is a flat potential, then Eq. (3) describes a simple 1D random walk. Both
 107 for $\alpha = 2$ and $\alpha \neq 2$, we then have time-reversal symmetry. If one were to make a
 108 movie of the moving particle, it would afterwards not be possible to determine whether
 109 the movie is played forward or backward. However, when the Brownian particle is
 110 in a 1D potential well, a different situation arises. When subjected to white Gaussian
 111 noise, Onsager’s microscopic reversibility has to apply, i.e., we still have time-reversal
 112 symmetry. But for a Lévy-noise-subjected particle in a 1D potential well, time-reversal
 113 symmetry is violated. Below we will explain this violation and elaborate on it. Based
 114 on the developed insights, we will formulate a measure for the time-reversal-symmetry
 115 breaking and we will derive approximate FDR relations for a nonequilibrium bath.

116 Consider the situation with the parabolic well, $V(x) = \frac{1}{2}Ax^2$ with $A > 0$, as
 117 depicted in Fig. 1a. Let the Brownian fluctuations make the particle go up the parabola to
 118 a considerable height x_0 outside the basin of attraction. As the basin of attraction of the
 119 potential we take the interval around the minimum where the particle spends around
 120 90% of its time. In case of Gaussian noise we have microscopic reversibility. The most
 121 likely Brownian kick has magnitude zero. Therefore the most likely downslide is a series
 122 of such ‘zero’ kicks and the most likely upslide is, perhaps unintuitively, the exact reverse.
 123 The deterministic downslide follows $\beta\dot{x} = -Ax$. This leads to $x(t) = x_0 \exp[-At/\beta]$.
 124 If we let the downslide run from x_0 all the way back back to $x = 0$, then we have
 125 for the dissipated energy $\int \beta\dot{x}(t) dx(t) = \beta \int_0^\infty \dot{x}^2 dt = (\beta^2/(2A))x_0^2$. In principle, the
 126 downslide to $x = 0$ takes infinitely long. But if we take as the endpoint a location x_* in the
 127 basin of attraction, then we have for the time t_* to reach x_* : $t_* = \beta \log[x_0/x_*]/A$. With
 128 a discretized time, this corresponds to $n = t_*/(\Delta t) = (\beta \log[x_0/x_*])/(A\Delta t)$ timesteps.

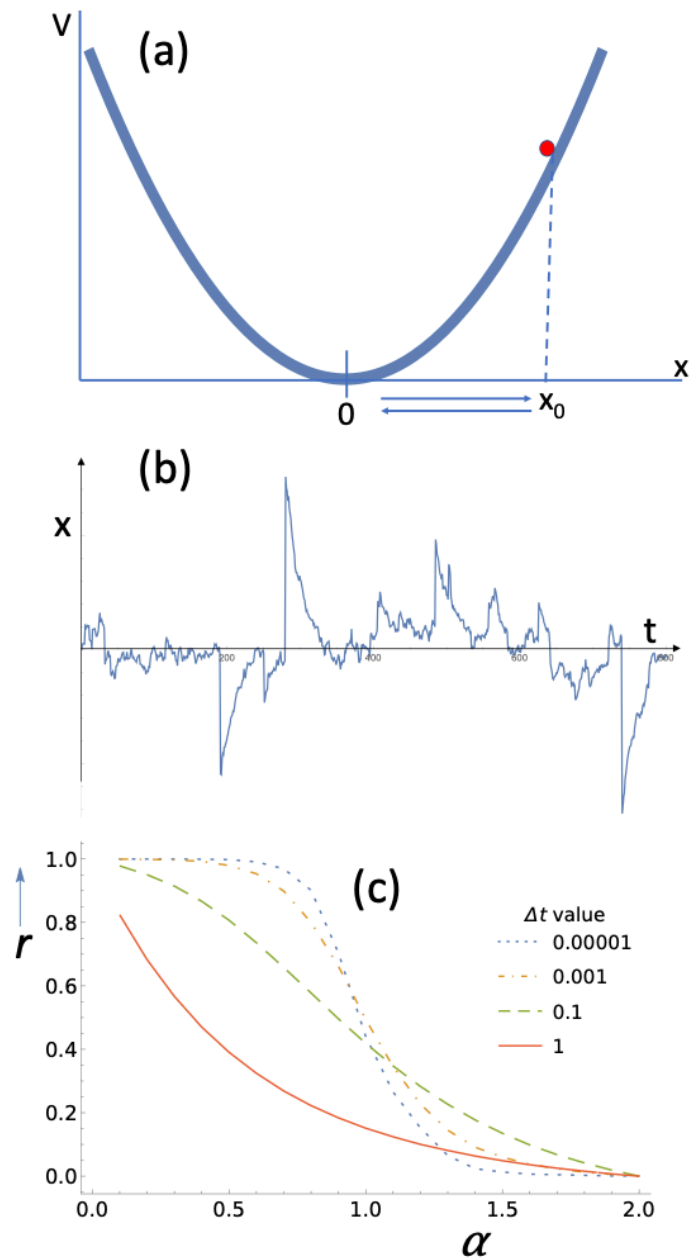


Figure 1. (a) A Brownian particle in a parabolic potential $V(x) = x^2/2$. (b) When subjected to Lévy noise ($\alpha = 1.5$, $c = 1$), microscopic reversibility, i.e. time-reversal symmetry, no longer applies. It is obvious from the figure that Lévy jumps lead to the particle “shooting up.” After the jump there is a slower relaxation, a “sliding down,” back to the basin of attraction. (c) The parameter r (see text) is a measure for the time-reversal asymmetry. The figure shows how r depends on the stability index α of the Lévy noise. There appears to be a smooth approach to $r = 0$ (time-reversal symmetry) as α approaches 2 (Gaussian noise). Δt represents the time interval taken in a Langevin simulation.

129 With Gaussian noise, the most likely upslide and most likely downslide both take n
 130 steps. In Ref. [22] it is shown rigorously that in case of Lévy noise, the most likely upslide
 131 takes one step and the most likely downslide takes n steps. Given what is observed in
 132 Fig. 1b, it is not hard to intuit this apparent violation of time-reversal symmetry. The
 133 noisy particle will spend most of its time in the basin of attraction near the bottom of the
 134 well. A Lévy jump makes the particle “shoot up” in one step. Afterwards it will slide
 135 down as if in equilibrium. Doing the upslide in one step (i.e. doing it n times as fast as

136 the deterministic downslide) leads to the dissipation of n times as much energy. This can
 137 be readily seen from the integral that gives the dissipated energy: $E_{diss} = \int \beta \dot{x}(t) dx(t)$.

138 Figures 1b affirms the insight formulated in the previous paragraph. The one-step
 139 Lévy jumps are conspicuous and so are the slower subsequent relaxations back to the
 140 bottom of the well.

141 For a potential with curvature, there is a problem when simulating the motion of
 142 a particle that is subjected to Lévy noise. Imagine that the particle in Fig. 1a is to the
 143 left of $x = 0$ and imagine next that it receives a large Lévy kick to the right. In a simple
 144 Euler scheme with a timestep Δt , we would have the deterministic force on the particle,
 145 $F(x) = -dV(x)/dx$, be in the positive direction for the entire interval, even when the
 146 particle is actually “climbing” the potential on the part of the potential where $x > 0$.
 147 For a parabolic potential the solution to this “large kick problem” is straightforward.
 148 Through scaling of t and x , the Langevin Equation $\beta \dot{x} = -Ax + \beta c \zeta_\alpha(t)$ can be brought
 149 into a form $\dot{x} = -\lambda x + \zeta_\alpha(t)$ [23]. We take $\lambda = 1$. Upon discretization of $\dot{x} = -x + \zeta_\alpha(t)$,
 150 we let the kick at $t = t_i$ have a value $\zeta_\alpha(t_i) = K$. We then take the curvature of the
 151 potential into account by simply taking the solution of $\dot{x} = -x + K$ as describing what
 152 occurs between $x(t_i) = x_i$ and $x(t_{i+1}) = x_{i+1}$. This leads to $x_{i+1} = (x_i - K)e^{-\Delta t} + K$.
 153 Figures 1b and 1c were obtained using the latter expression at every timestep.

After taking the data from a computer simulation (with a time interval Δt) or from
 a real life system (sampled at a time interval Δt), we can express the deviation from
 microscopic reversibility as follows:

$$r = \varphi_{\text{desc}} - \varphi_{\text{asc}}, \quad (6)$$

154 where φ_{desc} and φ_{asc} are the fraction of descending steps and the fraction of ascending
 155 steps, respectively. Descending steps are steps for which $V(x)|_{x_i}^{x_{i+1}} < 0$ and ascending
 156 steps are steps for which $V(x)|_{x_i}^{x_{i+1}} > 0$ (cf. Eq. (4)). Time-reversal turns ascending steps
 157 into descending steps and descending steps into ascending steps. So it is obvious that
 158 $r = 0$ in case of microscopic reversibility. No arrow of time can exist at equilibrium and
 159 $r = 0$ must ensue for any system at equilibrium. The parameter r indicates the level of
 160 symmetry breaking and can be thought of as an order parameter. Gaussian noise ($\alpha = 2$)
 161 leads to $r = 0$ on any shape potential, even if the potential is not a simple well.

162 Figure 1c shows r as a function of the stability index α for a Lévy-noise-subjected
 163 particle in a parabolic potential. Curves are drawn for different values of the time interval
 164 Δt . For Lévy noise there is a power-law-tail and a divergent variance for any $\alpha = 2 - \varepsilon$,
 165 where ε is small and positive. For $\alpha = 2$ the Gaussian is recovered. Nevertheless, the
 166 convergence to $r = 0$ as α approaches 2 appears smooth.

167 From Fig. 1c it is also obvious that there is a strong dependence on the timestep Δt .
 168 It is for the green curve in Fig. 1c, i.e. $\Delta t = 0.1$, that we get the fastest departure from
 169 $r = 0$. This apparent optimum is not hard to understand. In a parabola $V(x) = \frac{1}{2}Ax^2$ the
 170 deterministic downslide starting at $x_0 = x(t = 0)$ is described by $x(t) = x_0 \exp[-At/\beta]$.
 171 In other words, there is a characteristic time $t_{\text{char}} = \beta/A$ for the downslide. If $\Delta t \gg t_{\text{char}}$,
 172 then the particle will generally be back in the basin of attraction after one timestep.
 173 The shooting up and sliding down will not be resolved in that case. Suppose next that
 174 $\Delta t \rightarrow 0^+$. With $\beta \Delta x_i = -Ax_i \Delta t + \beta c \theta_i (\Delta t)^{1/\alpha}$ and $1 < \alpha < 2$, we then have $\Delta t^{1/\alpha} \gg \Delta t$.
 175 This leads to the noise-term being dominant and the contribution due to the slope being
 176 negligible. What this means in practice for the downslide is that it will take a very
 177 large number of steps, N_{tot} , to get back to the basin of attraction after a Lévy jump. A
 178 number $N_{\text{asc}} \approx N_{\text{tot}}/2$ of these steps will be ascending and a number $N_{\text{desc}} \approx N_{\text{tot}}/2$
 179 will be descending. The difference $N_{\text{desc}} - N_{\text{asc}}$ will be small relative to N_{tot} and will
 180 lead to $r = (N_{\text{desc}} - N_{\text{asc}})/N_{\text{tot}} \rightarrow 0$. In between $\Delta t \rightarrow 0^+$ and $\Delta t \gg t_{\text{char}}$ there will be
 181 a maximum for the value of r . Figure 1c shows that with a timestep, Δt , that is about
 182 one tenth of the characteristic time, t_{char} , an optimal resolution of the nonequilibrium
 183 features is obtained. The parameter r for a Lévy particle in a harmonic potential is further
 184 explored in Ref. [23].

185 “... when all the fast things have happened, but the slow things have not.” That is how
 186 Richard Feynman once described equilibrium [24]. The observations in the previous
 187 paragraph on the Lévy particle’s relaxation to the basin of attraction put an interesting
 188 take on Feynman’s premise for the case of our nonequilibrium system. If we take
 189 $\Delta t \gg t_{\text{char}}$ we are indeed not sampling sufficiently fast to see the relaxation happen and
 190 we are then looking at the $r = 0$ that characterizes equilibrium. But if we take $\Delta t \ll t_{\text{char}}$,
 191 we are sampling *too fast* and also do not see the relaxation happen as sampling too fast
 192 likewise leads to $r = 0$, i.e. the equilibrium result. So “... when the fast things happen, but
 193 we are sampling too fast to see it” would also describe equilibrium.

194 4. Corrections on the FDR for a small Deviation from Microscopic Reversibility

195 As we saw earlier, with Gaussian noise time-reversal symmetry implies that ascent
 196 and descent are on average equally fast. With Lévy noise the most likely trajectory from
 197 the basin of attraction to a position x_0 high above the minimum takes one timestep. The
 198 subsequent most likely descent follows the deterministic pattern that would also ensue
 199 if there were equilibrium. Below we analyze such breaking of time-reversal symmetry
 200 in a close-to-equilibrium condition. We will come to an intuitive understanding and
 201 associated approximate relations. Ultimately, we will derive how the FDR looks for a
 202 small deviation from equilibrium.

Consider a small interval Δx_0 on the x -axis. With a coefficient of friction β , the energy that is dissipated if Δx_0 is crossed at a speed v is $E = \beta v(\Delta x_0)$. Over a long time interval, Δx_0 is traversed equally often in both directions. Let v_0 be the speed on the downslide and let $v_0(1 + \delta)$ be the speed on the upslide. Close-to-equilibrium means that δ is sufficiently small to justify a first order approximation. With the upslide speed corrected by a multiplicative factor $(1 + \delta)$, the number of ascending steps gets a multiplicative factor $(1 - \delta)$ relative to the number of descending steps. This leads to:

$$r = \frac{N_{\text{desc}} - N_{\text{asc}}}{N_{\text{desc}} + N_{\text{asc}}} = \frac{1 - (1 - \delta)}{1 + (1 - \delta)} \approx \frac{1}{2} \delta. \quad (7)$$

If Δx_0 is traversed first at an upslide-speed $v_0(1 + \delta)$ and next, on the way back to the basin of attraction, at a speed v_0 , then the dissipated energy is:

$$E_{\text{diss}}^{\text{noneq}} = \beta v_0(1 + \delta)(\Delta x_0) + \beta v_0(\Delta x_0) = 2\beta v_0(\Delta x_0)(1 + r). \quad (8)$$

The energy $E_{\text{diss}}^{\text{eq}} = 2\beta v_0(\Delta x_0)$ is what would be dissipated if, in case of microscopic reversibility, we traverse the two directions with the same speed v_0 . The higher speeds on the upslides, i.e. the violation of microscopic reversibility, lead to the $(1 + r)$ correction factor:

$$E_{\text{diss}}^{\text{noneq}} = E_{\text{diss}}^{\text{eq}}(1 + r). \quad (9)$$

For a corrected Energy-FDR we thus find:

$$P_{\text{diss}}^{\text{noneq}} = \frac{2k_B T^{\text{eq}}}{\Delta t}(1 + r). \quad (10)$$

203 This equation can be seen as an adjusted form of Eq. (5) for the case of a small violation
 204 of time-reversal-symmetry as quantified by the parameter r . Note that the temperature
 205 T^{eq} is still in the formula. On the right-hand-side, the small r leads to a small amount of
 206 extra power being “fluctuated in.” This power is included in what gets dissipated.

In principle, temperature is a characteristic of a system that is at thermodynamic equilibrium. Nevertheless, even in a nonequilibrium setup, we can associate the temperature with the average kinetic energy of the particles, i.e., $\langle E_{\text{kin}} \rangle = \frac{1}{2}k_B T$ in case of a 1D system. Let upslide and downslide cover the same distance Δx_0 . In that case the upslide speed, $v_{\text{up}} = v_0(1 + \delta)$, is held for a shorter time than the downslide speed v_0 . This will lead to the average actually being smaller than $v_0(1 + \frac{1}{2}\delta)$. However, this is a second

order effect in δ (see the short derivation in the Appendix). At first order we thus have: $v_{\text{avg}} \approx v_0(1 + \frac{1}{2}\delta) = v_0(1 + r)$. If all of the involved particles have the same mass m and taking the average of the square as the square of the average, we come to a lowest order approximation: $\langle E_{\text{kin}} \rangle = \frac{1}{2}mv_{\text{avg}}^2 \approx \frac{1}{2}mv_0^2(1 + \delta)$. With $\delta = 2r$, this leads to

$$T^{\text{noneq}} = T^{\text{eq}}(1 + 2r). \quad (11)$$

The Kubo relation expresses the diffusion coefficient D as the time correlation of the velocity: $D = \int_0^\infty \langle v(t)v(0) \rangle dt$ [25]. With the insights developed in this paragraph we find that this leads to

$$D^{\text{noneq}} = D^{\text{eq}}(1 + 2r). \quad (12)$$

207 Equations (11) and (12) express, in terms of r , what the effect of the time-reversal-
 208 symmetry breaking is on the temperature and the diffusion. Equations (10-12) constitute
 209 the main result of this work.

210 5. A Stochastic Simulation with an Artificial Violation of Microscopic Reversibility

211 In this section we view the violation of time-reversal symmetry from a different
 212 perspective. We rederive Eqs. (11) and (12) and check the theoretical results with a
 213 stochastic simulation.

214 Consider Fig. 2. We take two points, P_1 and P_2 , on the parabolic potential of Fig. 1a.
 215 The point P_1 is in the basin of attraction and the distance between the points is such that
 216 it takes more than one timestep to cover the trajectory. Say it would take n steps to go
 217 from P_2 to P_1 on a deterministic downslide. As discussed before, at equilibrium the most
 218 likely upslide trajectory is the reverse of the deterministic downslide and also takes n
 219 steps. With the violation of microscopic reversibility that was discussed in the previous
 220 section, a mismatch arises. If the upslide speeds carry a factor $(1 + \delta)$, then the n steps
 221 will bring the particle further up in the potential. Instead of the equilibrium distance Δx ,
 222 a distance $\Delta x(1 + \delta)$ would be covered and the point P'_2 would be reached.

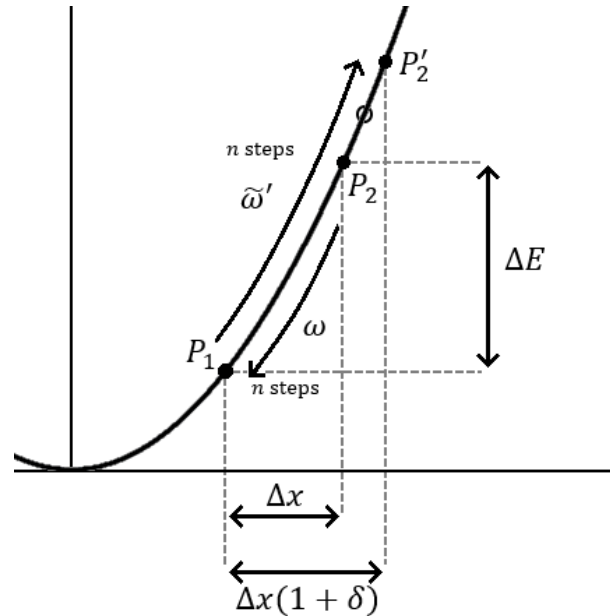


Figure 2. The parabolic potential with a point P_1 in the basin of attraction and a point P_2 significantly higher. At equilibrium, the upward trajectory $\tilde{\omega}$ and its reverse ω are traversed equally often. With a small violation of time-reversal symmetry, i.e. $r > 0$ and a slightly faster upslide, a mismatch arises. The adjusted upslide $\tilde{\omega}'$ reaches to P'_2 and the Boltzmann distribution in the potential is correspondingly widened.

For the equilibrium situation, there is an elegant relation connecting any trajectory ω to its time-reverse $\tilde{\omega}$. Let $P(\omega)$ and $P(\tilde{\omega})$ be the probabilities of the underlying sequences of steps for ω and $\tilde{\omega}$. We have [26]:

$$\frac{P(\tilde{\omega})}{P(\omega)} = \exp\left[-\frac{\Delta E}{k_B T}\right]. \quad (13)$$

223 The right-hand-side of the equation is recognized as the Boltzmann factor, i.e. the ratio
 224 of the population densities at P_2 and P_1 . With Eq. (13) we see that upslide and downslide
 225 ultimately occur equally often, i.e. we have microscopic reversibility.

226 With the small deviation from microscopic reversibility, we obtain the slightly
 227 mismatched situation: the starting point of the trajectory ω is a small distance away
 228 from the endpoint of $\tilde{\omega}'$. What is a single point P_2 in the equilibrium state, is a small
 229 segment at nonequilibrium. It is not unreasonable to hypothesize that the value of the
 230 probability density that at equilibrium corresponds to P_2 is achieved halfway between
 231 P_2 and P_2' at nonequilibrium. This point is indicated in Fig. 2 with an open circle.

232 It is obvious that the augmentation of the upsides (cf. Fig. 2) leads to a widening
 233 of the distribution. The standard deviation will increase, but it will not become infinite
 234 as with α -stable distributions. In other words, we move towards the $\alpha < 2$ situation
 235 without blowing up the standard deviation and other moments.

236 With Eq. (3) and Gaussian noise, the stationary probability distribution for the
 237 position in a parabolic potential $V(x) = \frac{1}{2}Ax^2$ is a zero-average Gaussian with a standard
 238 deviation of $\sigma = \sqrt{D/A}$ [1]. With the small violation of microscopic reversibility
 239 characterized by δ , we expect that the probability density will still “look” very Gaussian,
 240 but it will have a standard deviation of $\sigma' = \sigma(1 + \delta/2) = \sigma(1 + r)$ (cf. Fig. 2). So the
 241 Gaussian will be stretched by a multiplicative factor $(1 + r)$.

242 With $\sigma = \sqrt{D/A}$, we see that \sqrt{D} gets a multiplicative factor $(1 + r)$ upon going to
 243 nonequilibrium. This means that D gets, at first order, a factor $(1 + 2r)$, i.e. we retrieve
 244 Eq. (12). With the FDR, $D = k_B T / \beta$, we see that Eq. (11) follows concurrently.

245 The ideas put forward in the previous paragraphs can be readily checked through
 246 a Langevin simulation. The simulation is based on a Euler scheme using Eq. (3). The
 247 coefficient of friction β and the diffusion coefficient D are set equal to one and we
 248 also pick $A = 1$. The Euler scheme thus computes the increments and new positions
 249 using $\Delta x_i = -x_i \Delta t + \theta_{2,i} \sqrt{2\Delta t}$ and $x_{i+1} = x_i + \Delta x_i$, respectively, where $\theta_{2,i}$ is the i -th
 250 random number drawn from a Gaussian distribution with a zero-average and a standard
 251 deviation of one. A breaking of time-reversal symmetry similar to the one brought about
 252 by Lévy jumps is applied by simply augmenting the climbing steps by a small fraction
 253 δ . However, care must be taken here as $\sigma' = \sigma(1 + \delta/2)$ is only obtained when some
 254 supplementary conditions are implemented.

255 Following the simple criterion for “climbing” formulated with Eq. (6), the augmen-
 256 tation would also apply inside the basin of attraction. This would lead to the Gaussian
 257 distribution becoming bimodal, i.e., the distribution turning into one with two
 258 maxima. Bimodal distributions have been observed more commonly in the context of
 259 Lévy noise in a potential well [27–29]. The bimodality is intriguing and worth further
 260 study, but here we wish to stop it from occurring and maintain the Gaussian shape.
 261 We thus only apply the augmentation outside the basin of attraction, i.e. on the i -th
 262 step if $|x_i| > \hat{x}$ and $\text{sgn}(\Delta x_i) = \text{sgn}(x_i)$. With this procedure we “fatten” the tail of the
 263 position distribution without causing bimodality or bringing about an infinite standard
 264 deviation. Figure 3 shows how for $\hat{x} = 1.87$, i.e. almost two standard deviations from the
 265 center, we obtain the $\sigma' = (1 + \delta/2)$ that the theory predicts. For a Gaussian distribution
 266 with a unit standard deviation, the interval between -1.87 and 1.87 contains 94% of the
 267 probability.

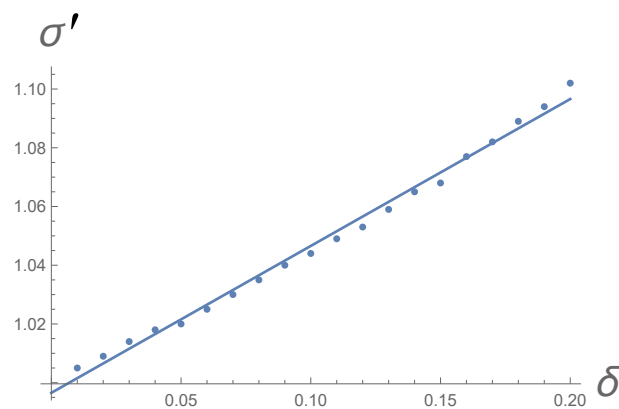


Figure 3. Each point is the result of a Langevin simulation of 125 million steps. The line represents the best linear fit to the points. The basic setup is that of a Euler scheme following a Brownian particle in a parabolic potential $V(x) = x^2/2$. We take $\beta = 1$ and $D = 1$ (see text). The timesteps have a length of $\Delta t = 0.01$. The breaking of microscopic reversibility consists in an augmentation of climbing steps that occur at more than 1.87 standard deviations away from $x = 0$. The parameter δ , which is varied from 0.01 to 0.2 in steps of 0.01, represents the fraction by which a climbing step is made longer. We let σ' represent the standard deviation of the augmented Gaussian. The graph shows how the simulations bear out the theoretically derived $\sigma' = (1 + \delta/2)$.

268 6. Discussion

269 Extension of the FDR to nonequilibrium is a challenge that has been taken up by
 270 many and different approaches have been tried [10,30,31]. Our starting point is a Lévy-
 271 noise-subjected particle in a quadratic potential well. The quadratic potential well is
 272 generic in the sense that along any potential profile $V(x)$, the first term in the expansion
 273 around a minimum at $x = x_0$ is generally quadratic, i.e. $V(x) \approx V(x_0) + \frac{1}{2}V''(x_0)(x -$
 274 $x_0)^2$.

275 Lévy noise is characterized by the occurrence of frequent outliers. In everyday
 276 data-processing practice, however, the reasoning is often in the opposite direction: upon
 277 observation of frequent outliers it is inferred that the underlying noise must be Lévy.
 278 Subsequent theoretical analysis is then commonly greatly impaired by the divergent
 279 integrals that are associated with Lévy noise. In the face of these infinities, relating data
 280 and theory is no longer straightforward.

281 At that point it makes sense to take a step back and realize that infinity is an
 282 abstraction. In the aforementioned setup of Kanazawa et al [11], for instance, the liquid
 283 in an experimental realization has to be in a container and it is obvious that no Lévy
 284 jump will ever be larger than the size of the container. Silva et al [17] followed the spatial
 285 fluctuations of a cytoskeletal network and found fat tails in the ensuing distribution.
 286 Also here the container size imposes a natural cutoff on the jump size. An infinite
 287 standard deviation is just as unrealistic as $\Delta t \rightarrow 0$ in our Eq. (5).

288 With finite standard deviations the Central Limit Theorem should apply again.
 289 This idea was what motivated Mantegna and Stanley as they took n different truncated
 290 α -stable distributions [32]. They added the results of draws from these n distributions
 291 and found that convergence to a Gaussian occurs with increasing n , but it is very slow.
 292 Note that the position distribution that we arrive at in Section 5 is still Gaussian, but that
 293 it has just been artificially widened by the augmentation of the climbing steps.

294 In this article we started with the observation that time-reversal-symmetry is vio-
 295 lated for a Lévy-noise-subjected particle in a harmonic well. The particle tends to “shoot
 296 up” and “slide down.” We quantified the “degree of violation” with a parameter r . For
 297 the Lévy-noise-subjected particle in a harmonic well, the standard deviation and the
 298 higher moments diverge. There is no temperature and no FDR. We devised a way to
 299 artificially implement a small amount of violation of the time-reversal-symmetry. In this
 300 Discussion section we explained why it is sensible and realistic to keep all the involved

301 moments finite. Our scheme does not give rise to divergent integrals and leads to simple
 302 expressions for a corrected FDR. The correction only involves the parameter r .

303 A possible experimental verification of Eqs. (10) and (12) would entail a setup
 304 with an energy input; an energy input leading to a bath with particles whose motion
 305 violates time-reversal-symmetry. Through following that motion with a probe, the r
 306 could possibly be established. The power dissipation or the diffusion coefficient could
 307 next be established independently.

308 **Author Contributions:** Conceptualization, S.Y. and M.B.; methodology, S.Y., N.B. and M.B; soft-
 309 ware, S.Y. and N.B.; formal analysis, S.Y., N.B. and M.B; investigation, S.Y., N.B. and M.B; writing—
 310 original draft preparation, N.B. and M.B.; writing—review and editing, S.Y., N.B. and M.B;
 311 supervision, M.B. All authors have read and agreed to the published version of the manuscript.

312 **Funding:** This research received no external funding.

313 **Conflicts of Interest:** The authors declare no conflict of interest.

314 Abbreviations

315 The following abbreviations are used in this manuscript:

316 FDR Fluctuation-Dissipation Relation

IID Independent and Identically Distributed

317 Appendix A

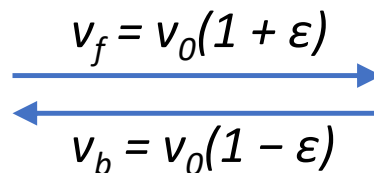
318 Consider the situation depicted in Fig. A1. An interval Δx is traversed at a speed
 319 $v_f = v_0(1 + \varepsilon)$ and next at a speed $v_b = v_0(1 - \varepsilon)$ in the reverse direction. The total time
 320 for the out-and-back run is

$$\begin{aligned} T_{tot} &= \frac{\Delta x}{v_f} + \frac{\Delta x}{v_b} \\ &= \frac{\Delta x}{v_0} \left(\frac{1}{1 + \varepsilon} + \frac{1}{1 - \varepsilon} \right) \\ &\approx \frac{2\Delta x}{v_0} (1 + \varepsilon^2). \end{aligned}$$

Fourth and higher order contributions have been neglected in the last expression. For the average speed over the entire out and back trajectory, we now have

$$v_{avg} = \frac{2\Delta x}{T_{tot}} \approx v_0(1 - \varepsilon^2).$$

321 We see that the average speed, v_{avg} , is lower than v_0 . This is due to the fact that the lower
 322 speed is held over the same distance as the higher speed. It is therefore kept for a longer
 323 time than the higher speed. The first correction on v_0 is quadratic in ε . For the first order
 324 treatment in Section 4, the second-order-correction can be disregarded.



$$\begin{array}{c} \xrightarrow{v_f = v_0(1 + \varepsilon)} \\ \xleftarrow{v_b = v_0(1 - \varepsilon)} \end{array}$$

Figure A1. An interval of length Δx is traversed in the forward direction at a speed $v_f = v_0(1 + \varepsilon)$ and, subsequently, in the backward direction at a speed $v_b = v_0(1 - \varepsilon)$. In this Appendix it is shown that the average speed during the out-and-back run is v_0 with a lowest order correction that is quadratic in ε : $v_{avg} = v_0(1 - \varepsilon^2)$.

References

1. van Kampen, N.G. *Stochastic Processes in Physics and Chemistry*; Elsevier: Amsterdam, the Netherlands, 1992.
2. Bier, M.; Weaver, J.C. Signals, Noise, and Thresholds. In *CRC Handbook of Biological Effects of Electromagnetic Fields - Bioengineering and Biophysical Aspects of Electromagnetic Fields*, 4th ed.; Greenebaum, B., Barnes, F.S., Eds.; CRC Press - Taylor and Francis Group: Boca Raton FL, USA, 2019; pp. 261-298.
3. Kubo, R. *Rep. Prog. Phys.* **1966**, *29*, 255-284.
4. Onsager, L. Reciprocal Relations in Irreversible Processes. I. *Phys. Rev.* **1931**, *37*, 405-426.
5. Onsager, L. Reciprocal Relations in Irreversible Processes. II. *Phys. Rev.* **1931**, *38*, 2265-2279.
6. Jarzynski, C. Nonequilibrium equality for free energy differences. *Phys. Rev. Lett.* **1997**, *78*(14), 2690-2693.
7. Jarzynski, C. Equilibrium free-energy differences from nonequilibrium measurements: A master-equation approach. *Phys. Rev. E* **1997**, *56*(5), 5018-5035.
8. Liphardt, J.; Dumont, S.; Smith, S.B.; Tinoco Jr., I.; Bustamante, C. Equilibrium Information from Nonequilibrium Measurements in an Experimental Test of Jarzynski's Equality. *Science* **2002**, *296*(5574), 1832-1835.
9. Hatano T.; Sasa, S.-i. Steady State Thermodynamics of Langevin Systems. *Phys. Rev. Lett.* **2001**, *86*, 3463-3466.
10. Baiesi, M.; Maes, C.; Wynants, B. Fluctuations and response of nonequilibrium states. *Phys. Rev. Lett.* **2009**, *103*, 010602.
11. Kanazawa, K.; Sano, T.G.; Cairoli, A.; Baule, A. Loopy Lévy flights enhance tracer diffusion in active suspensions. *Nature* **2020**, *579*, 364-367.
12. Mandelbrot, B. The Variation of Certain Speculative Prices *J. Bus.* **1963**, *36*(4), 394-419.
13. Mandelbrot, B. *The Fractal Geometry of Nature*; W.H. Freeman: San Francisco, USA, 1983.
14. Burnecki, K.; Wyłomańska, A.; Beletskii, A.; Gonchar, V.; Chechkin, A. Recognition of stable distribution with Lévy index α close to 2. *Phys. Rev. E* **2012**, *85*, 056711.
15. Rypdal M.; Rypdal K. Testing Hypotheses about Sun-Climate Complexity Linking. *Phys. Rev. Lett.* **2010**, *104*, 128501.
16. Peng, C.-K.; Mietus, J.; Hausdorff, J.M.; Havlin, S.; Stanley, H.E.; Goldberger, A.L. Long-range anticorrelations and non-Gaussian behavior of the heartbeat. *Phys. Rev. Lett.* **1993**, *70*, 1343-1346.
17. e Silva, M.S.; Stuhrmann, B.; Betz, T.; Koenderink, G.H. Time-resolved microrheology of actively remodeling actomyosin networks. *New J. Phys.* **2014**, *16*, 075010.
18. Klafter, J.; Shlesinger, M.F.; Zumofen, G. Beyond Brownian Motion. *Phys. Today* **1996**, *49*(2), 33-39.
19. Samorodnitsky, G.; Taqqu, M.S. *Stable Non-Gaussian Random Processes*; Chapman & Hall: London, UK, 1994.
20. Sekimoto, K. Langevin equation and thermodynamics. *Prog. Theor. Phys. Supplement* **1998**, *130*, 17-27.
21. Sekimoto, K.; Sasa, S.-i. Complementarity Relation for Irreversible Process Derived from Stochastic Energetics. *J. Phys. Soc. Jpn.* **1997**, *11*(66), 3326-3328.
22. Kuśmierz, Ł.; Chechkin, A.V.; Gudowska-Nowak, E.; Bier, M. Breaking microscopic reversibility with Lévy flights. *Europhys. Lett.* **2016**, *114*, 60009.
23. Yuvan, S.; Bier, M.; The Breaking of Time-Reversal Symmetry for a Particle in a Parabolic Potential that is Subjected to Lévy Noise - Theory and an Application to Solar Flare Data. *Phys. Rev. E* **2021**, *104*, 014119.
24. Feynman, R.P. *Statistical Mechanics: A Set of Lectures*; Westview: Boulder, CO, USA, 1972.
25. Zwanzig, R. *Nonequilibrium Statistical Mechanics*; Oxford University Press: Oxford, UK, 2001, Chptr. 1, Sect. 2.
26. Bier, M.; Derényi, I.; Kostur, M.; Astumian, R.D. Intrawell relaxation of overdamped Brownian particles. *Phys. Rev. E* **1999**, *59*(6), 6422-6432.
27. Chechkin, A.V.; Klafter, J.; Gonchar, V.Yu.; Metzler, R.; Tanatorov, L.V. Bifurcation, bimodality, and finite variance in confined Lévy flights. *Phys. Rev. E* **2003**, *67*, 010102.
28. Chechkin, A.V.; Gonchar, V.Yu.; Klafter, J.; Metzler, R.; Tanatorov, L.V. Lévy flights in a steep potential well. *J. Stat. Phys.* **2004**, *115*(5/6), 1505-1535.
29. Capała K.; Dybiec, B. Multimodal stationary states in symmetric single-well potentials driven by Cauchy noise. *J. Stat. Mech.: Theory Exp.* **2019**, 2019 033206.
30. Prost, J.; Joanny, J.-F.; Parrondo, J.M.R. Generalized Fluctuation-Dissipation Theorem for Steady-State Systems. *Phys. Rev. Lett.* **2009**, *103*, 090601.
31. Dybiec, B.; Parrondo, J.M.R.; Gudowska-Nowak, E. Fluctuation-dissipation relations under Lévy noises. *Europhys. Lett.* **2012**, *98*(5), 50006.
32. Mantegna, R.N.; Stanley, H.E. Stochastic Process with Ultraslow Convergence to a Gaussian: The Truncated Lévy Flight, *Phys. Rev. Lett.* **1994**, *73*(22), 2946-2949.